Electron Cryomicroscopy of Bacteriorhodopsin Vesicles: Mechanism of Vesicle Formation

Nikolai D. Denkov,* Hideyuki Yoshimura,# Tsutomu Kouyama,§ Jochen Walz,¶ and Kuniaki Nagayama‖
*#‖ Protein Array Project, ERATO, JRDC, Tsukuba Research Consortium, Tsukuba 300-26, Japan; § Department of Physics, Faculty of Science, Nagoya University, Nagoya 464-01, Japan; and ¶ Max-Planck-Institut für Biochemie, 82152 Martinsried, Germany

ABSTRACT We obtained vesicles from purple membrane of *Halobacterium halobium* at different suspension compositions (pH, electrolytes, buffers), following the procedure of Kouyama et al. (1994) (*J. Mol. Biol.* 236:990–994). The vesicles contained bacteriorhodopsin (bR) and halolipid, and spontaneously formed during incubation of purple membrane suspension in the presence of detergent octylthioglucoside (OTG) if the protein:OTG ratio was 2:1 by weight. The size distribution of the vesicles was precisely determined by electron cryomicroscopy and was found to be almost independent on the incubation conditions (mean radius 17.9–19 nm). The size distribution in a given sample was close to the normal one, with a standard deviation of $\sim\pm1$ nm. During dialysis for removal of the detergent, the vesicles diminished their radius by 2–2.5 nm. The results allow us to conclude that the driving force for the formation of bR vesicles is the preferential incorporation of OTG molecules in the cytoplasmic side of the membrane (with possible preferential delipidation of the extracellular side), which creates spontaneous curvature of the purple membrane. From the size distribution of the vesicles, we calculated the elasticity bending constant, $K_B \approx 9 \times 10^{-20}$ J, of the vesicle wall. The results provide some insight into the possible formation mechanisms of spherical assembles in living organisms. The conditions for vesicle formation and the mechanical properties of the vesicles could also be of interest with respect to the potential technological application of the bR vesicles as light energy converters.

INTRODUCTION

As shown recently (Kouyama et al., 1994), closed shells (vesicles) spontaneously form from the purple membrane of *Halobacterium halobium* when the latter is incubated at elevated temperatures in the presence of a detergent, octylthioglucoside (OTG). Under certain conditions, the vesicles formed well-shaped hexagonal crystals of millimeter size. Atomic force microscopy and x-ray diffraction experiments showed that these crystals were composed of apparently monodisperse vesicles (radius ~25 nm), closely packed in a hexagonal three-dimensional array. However, the diffraction pattern revealed only the mean interparticle center-to-center distance, and another lattice constant, which was close to the unit cell size in the purple membrane. The latter result was interpreted as an indication that the trimeric structure of bacteriorhodopsin (bR) was retained in the vesicles, but the orientation of the trimers in the space was isotropic rather than crystalline. The photoactivity of the vesicles was studied, and the results led to the conclusions that 1) practically all of the bR molecules are oriented in the same direction (their cytoplasmic side facing the external medium), and 2) the vesicles contain some native lipid, which probably contributes to the stabilization of the protein aggregate. Transformations of the spherical vesicles into tubular and doughnut-like structures were observed (when the ionic strength of the aqueous medium was lowered) and discussed with respect to the mechanisms of morphological changes of some subcellular membranes.

That study (Kouyama et al., 1994) poses several questions that deserve further investigation. First it remains unclear what the driving force is for the spontaneous bending of the purple membrane that forms vesicles of such a high curvature (radius $\approx$ 25 nm). As known, the planar structure of purple membrane is very stable in aqueous solutions. Closed cell envelope vesicles from purple membrane can be obtained by sonication of *H. halobium* (see, e.g., Tributsch and Bogomolni, 1994), but their radius is typically one order of magnitude larger (~200 nm). Kouyama et al. (1994) also mentioned that closed vesicles could be obtained by sonication of purified purple membrane in the presence of salts and ether, but the efficiency of conversion was low. On the other hand, Tributsch and Bogomolni (1994) reported that reconstituted vesicles of bR could be formed (in the presence of purified azolectin lipids and the detergent octylglucoside) with radius $\approx$ 50 nm. Again, the orientation of the bR molecules in these smaller vesicles was unidirectional with respect to the plane of the membrane. Therefore, one could expect that the spontaneous formation of small vesicles (20–50 nm in radius) in the presence of detergents is a process that is rather different from the sonication procedure, which leads to much larger vesicles gripped in a meta-stable state.

Received for publication 22 August 1997 and in final form 1 December 1997.

Address reprint requests to Dr. Nikolai D. Denkov, Faculty of Chemistry, Sofia University, 1 James Bourchier Ave., 1126 Sofia, Bulgaria. Tel.: 359-2-9625310; Fax: 359-2-9625643; E-mail: denkov@ltph.bol.bg.

Dr. Yoshimura's present address is Department of Physics, School of Science and Technology, Meiji University, 1-1-1 Higashimata, Tama-ku, Kawasaki 214, Japan.

Dr. Nagayama's present address is National Institute for Physiological Sciences, Myodaiji-cho, Okazaki, 444, Japan.

© 1998 by the Biophysical Society

0006-3495/98/03/1409/12 $2.00

The revealing of the driving force of vesicle formation is of interest because it could give some insight in the mechanisms of formation of spherical protein assemblies in living nature. A number of proteins are able to form spherical aggregates in vivo: clathrin (Pearse and Crowther, 1987), coatomer complex (Kreis, 1992; Orci et al., 1993), riboflavin synthase (Ladenstein et al., 1988), and the proteins assembling in viral capsids (Caspar and Klug, 1962; Harrison, 1984; Branden and Tooze, 1991). Three well-known examples of the important role of protein-containing vesicles in eukariotic cells are the clathrin-coated vesicles that realize the endocytosis of ligands bound to the cell surface; the coatomer-coated vesicles that transport the proteins to and from the Golgi complex; and the synaptic vesicles in the nerve cells that transfer the neurotransmitters from the presynaptic cell into the synaptic cleft (Darnel et al., 1990; Alberts et al., 1994; Kelly, 1993). All of these types of protein-containing vesicles are of similar size (20–50 nm in radius), and the driving force of their formation is still a matter of discussion in the literature. Sometimes the curvature of protein-enriched membranes is explained by the two-dimensional aggregation of asymmetrical ("conical" in shape or peripheral) membrane proteins, but other explanations are also feasible (Israelachvili, 1977; Israelachvili et al., 1980). Therefore, studies of artificially synthesized, highly curved aggregates (such as the bR vesicles) could help one more deeply understand the processes of vesicle formation in living organisms.

As a rule, the vesicles in eukariotic cells, discussed above, are not monodisperse, and a substantial variation in the size of coexisting vesicles is usually observed. This is in great contrast to the fixed size of the capsids of quasispherical viruses. The proteins, building up the protein capsid, assemble in a very regular cage, which in its turn can be crystallized into three-dimensional (Klug and Caspar, 1960; Caspar and Klug, 1962) or two-dimensional crystals (Horne and Pasquali-Ronchetti, 1974; Horne, 1979). These crystals were very useful for the structural analysis of viruses by x-ray diffraction and electron microscopy. The three-dimensional (3D) arrays of bR vesicles, however, did not show diffraction patterns that allowed a search for any structural details (Kouyama et al., 1994). The reason for this poor diffraction pattern remained unclear. It could be due simply to the different orientation in the 3D array of otherwise identical in structure vesicles, but it could reflect also the possibility of a different structure of the vesicles in the array (despite their similar size).

The interest in the 3D crystallization of membrane proteins (Henderson and Shotton, 1980; Michel and Oesterhelt, 1980; Michel, 1982; Schertler et al., 1993; Kühlbrandt, 1988) is also created by the fact that the vertical resolution of the electron diffraction studies of tilted 2D protein crystals is lower than the lateral resolution, because of the so-called missing cone problem (Henderson and Unwin, 1975). Briefly, the specimen cannot be tilted by angles larger that ~60° because of technical constraints. The absence of data in the high tilting angle region (missing cone) reduces the resolution, especially in direction perpendicular to the 2D crystal plane. The problem could be overcome, in principle, if the protein molecules can be oriented in different directions with respect to the plane of the electron microscope grid (Sakata et al., 1992; Takeda et al., 1995). Therefore, the formation of a true 3D or 2D crystal composed of protein vesicles is one opportunity for overcoming the missing cone problem and to improve the resolution of the structural analysis.

Last but not least, the interest in bR vesicles is stimulated by their nontrivial photochemical activity. As shown by Oesterhelt and Stoeckenius (1973), bR acts as a light-driven proton pump in the photosynthesis performed by *H. halobium* (see also Khorana, 1988; Ebrey, 1993). The resulting pH gradient across the purple membrane is used by the bacteria to synthesize ATP. Quite recently Trubitsch and Bogomolni (1994) (see also Birge, 1994) discovered that the bR vesicles could create sustained periodical changes (oscillations) in the pH of the surrounding aqueous medium, when the suspension is illuminated with continuous light. According to the authors, these oscillations are evidence that bacteriorhodopsin incorporates a positive synchronized feedback in regulating its proton pumping activity. The molecular mechanism responsible for this complex behavior of the bR molecules is still unclear, although a great advance in the structural analysis of the molecules has been achieved (Henderson et al., 1990; Grigorieff et al., 1996; Kimura et al., 1997).

The aims of the present study are to further analyze the structure of the bR vesicles by electron cryomicroscopy, and to search for the driving force of the vesicle formation from the planar sheets of purple membrane. We vitrified thin aqueous films, containing vesicles, by ultrarapid freezing in cold cryogen liquid, and then observed the frozen samples by electron microscope at −190°C (Dubochet et al., 1988). This method is particularly appropriate for the investigation of soft molecular aggregates that are unstable when dried, like the bR vesicles, because vitrification ensures excellent structural preservation and no staining or fixation reagents are needed, which could affect or even disrupt the vesicle structure. The size distribution of the vesicles can be determined to very high precision. The results show that the bR vesicles have no regular structure, like that of the icosahedral viruses, although their size is much more uniform compared to the vesicles in eukariotic cells. To understand the mechanism of vesicle formation, we prepared a number of samples incubated at different conditions. As described below, the comparison of the size of the vesicles in these samples, along with some other results, allowed us to formulate a sound hypothesis about the driving force of the purple membrane transformation into vesicles.

The article is organized in the following way. The next section presents the experimental procedures; the third section describes the experimental results; in the section titled Mechanism of Vesicle Formation and Vesicle Structure, these results are discussed from the viewpoint of the mechanism of vesicle formation; in the section titled Bending

Constant of Nondialized bR Vesicles, we calculate the bending elasticity modulus of the vesicle membrane from the measured size distribution of the vesicles by using a thermodynamic approach. The conclusions are summarized at the end.

EXPERIMENTAL PROCEDURES

Preparation of the vesicles

The vesicles were prepared by following the procedure of Kouyama et al. (1994). Purple membrane from *H. halobium*, strain JW3, was purified as described by Oesterhelt and Stoeckenius (1974). After washing with 0.17% Tween 20 (Fukuda et al., 1990), the purple membrane (2–5.8 mg/ml) was suspended in a solution of 2.3–9.3 mM octylthioglucoside (OTG), buffer (citrate, phosphate, or HEPES), electrolytes (0.22 or 0.4 M NaCl and 0–1.25 M ammonium sulfate), and 0.05% NaN_3. The composition of the original suspension for each of the studied samples is specified in Table 1. Briefly, samples 1–3 were incubated in the presence of 1 M ammonium sulfate (AS) and 0.4 M NaCl at different pH (5.2, 6.4, and 7.7, maintained by citrate, phosphate, and HEPES buffers, respectively). Samples 4–6 were incubated in the presence of 0.4 M NaCl (without AS) at pH 5.2 (maintained by phosphate or citrate buffer) and 6.4 (phosphate buffer). Samples 7 and 8 were incubated in the presence of 0.22 M NaCl and 1.25 M AS at higher pH (pH 8, maintained by HEPES).

Two-milliliter aliquots of these suspensions were incubated at 32°C for at least 5 days (see Fig. 1). After the incubation period, the samples were centrifuged at 4000 rpm for 40 min to remove the formed precipitate of irregularly stacked membranes. By electron microscopy we found that the remaining supernatant liquor contained closed spherical shells of purple membrane of radius 20–25 nm. For brevity, hereafter we will call the closed shells of purple membrane bacteriorhodopsin vesicles (bR vesicles).

To remove the excess of OTG and electrolytes from the bR suspensions, the latter were dialyzed in two stages against electrolyte solutions of lower concentrations. The composition of the used solutions depended on the composition of the original suspension (see Table 1):

Procedure 1: (a) 0.5 M ammonium sulfate and 0.05 M phosphate buffer of pH 6.4;
(b) 0.1 M ammonium sulfate and 0.01 M phosphate buffer of pH 6.4.
Procedure 2: (a) 0.5 M phosphate buffer of pH 6.4;
(b) 0.1 M ammonium sulfate.
Procedure 3: (a) 0.5 M citrate buffer of pH 6.4;
(b) 0.1 M citrate buffer of pH 6.4.

TABLE 1 List of the studied samples

	Conditions of vesicle formation							
Sample code	Purple membr. (mg/ml)	OTG (mM)	pH	Buffer (mM)	AS (M)	NaCl (M)	Procedure of dialysis	Mean radius ± SD (nm)
1Nd	5	6.7	5.2	40 citrate	1	0.4	Nondialized	17.9 ± 0.9
1Dd	5	6.7	5.2	40 citrate	1	0.4	1	15.9 ± 1.1
1LD	2	4.6	5.2	40 citrate	1	0.4	1	15.7 ± 0.9
2Nd	5	6.7	6.4	100 phosph.	1	0.4	Nondialized	18.0 ± 1.1
2Dd	5	6.7	6.4	100 phosph.	1	0.4	1	15.7 ± 0.7
2LD	2	4.6	6.4	100 phosph.	1	0.4	1	15.7 ± 1.1
3Dd	5	6.7	7.7	80 HEPES	1	0.4	1	15.5 ± 0.8
4Nd	5	6.7	5.2	1000 phosph.	0	0.4	Nondialized	19.0 ± 1.2
4Dd	5	6.7	5.2	1000 phosph.	0	0.4	2	15.3 ± 1.0
4LD	2	2.3	5.2	1000 phosph.	0	0.4	2	16.4 ± 0.8
5Dd	5	6.7	6.4	800 phosph.	0	0.4	2	16.6 ± 1.1
6Nd	5	6.7	5.2	700 citrate	0	0.4	Nondialized	18.9 ± 1.1
6Dd	5	6.7	5.2	700 citrate	0	0.4	3	16.7 ± 1.2
7Dd	5.8	7.0	8.0	100 HEPES	1.25	0.22	1	14.9 ± 0.8
8Dd	5.8	9.3	8.0	100 HEPES	1.25	0.22	1	14.7 ± 1.1

The number (1–8) in the sample code denotes the composition of the suspension during incubation; the letter Nd means that the sample is nondialyzed; the abbreviation Dd means that the sample is dialyzed; the abbreviation LD means that these are dialyzed samples obtained after incubation at lower OTG and purple membrane concentrations. AS means ammonium sulfate. The procedures for dialysis are described in the text. The last column contains the mean radius and the standard deviation, obtained from the size distribution of the vesicles in the given sample, as explained in the text. The quoted radius is defined with respect to the darkest portion of the vesicle contour. The outer radius of the vesicle is ~2.25 nm larger.

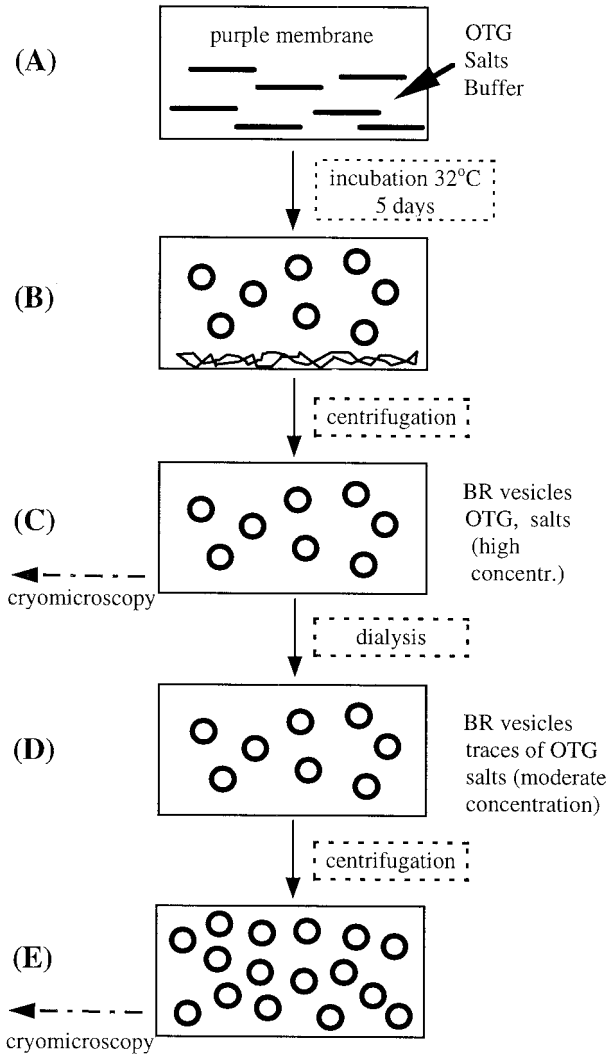

FIGURE 1 Schematic presentation of the procedures for sample preparation (Kouyama et al., 1994). (*A*) The bR vesicles were spontaneously forming during the incubation of purple membrane at 32°C in the presence of detergent octylthioglucoside (OTG), electrolytes, and buffers. (*B*) Along with the vesicles, a precipitate of irregularly stacked membranes formed, and it was removed by soft centrifugation. (*C*) The purified suspension of vesicles was studied by electron cryomicroscopy, or it was dialyzed for removal of OTG and to decrease the electrolyte concentration. (*D*) The concentration of bR in the dialyzed samples was measured spectrophotometrically, and the suspensions were concentrated by ultracentrifugation. (*E*) The final concentration of 0.22 mg/ml bR was most suitable for electron cryomicroscopy.

The samples were centrifuged at 10,000 rpm for 20 min to remove the small precipitate formed during the dialysis.

The dialyzed samples contained bR vesicles, traces of OTG, and electrolytes of moderate concentration. The concentration of bR in the dialyzed suspensions was determined by measuring the light absorption in a UV-visible spectrophotometer (UV-240; Shimadzu, Japan) at light wavelength (λ = 568 nm). By using the value of the molar extinction of the light-adapted bR monomer ($\epsilon_{568} = 6.3 \times 10^4\ M^{-1}\ cm^{-1}$; Rehorek and Heyn, 1979), we calculated the bR concentration from the measured light absorption. Finally, the samples were concentrated to reach the desired concentration of 8.7×10^{-4} M monomers (0.22 mg/ml bacteriorhodopsin), which was most suitable for the electron cryomicroscopy study (see below). The samples were concentrated by ultracentrifugation at 50,000 rpm for 1 h at 18°C (Beckman TL-100 ultracentrifuge, rotor type TLA 100.2). The excess of the colorless supernatant was removed, and the sediment of concentrated vesicles was kept at rest for several hours to ensure the spontaneous spreading of the vesicles throughout the suspension without mechanical agitation. These suspensions were very stable over time, and no visible changes were detected over months of shelf storage.

Electron cryomicroscopy

The preparation of vitrified samples for electron cryomicroscopy was performed by the method for controlled formation of vitrified films developed recently (Denkov et al., 1996a). The procedure included the formation of a single, relatively large diameter (50–100 μm) water-in-air film in the central hole of a disc-shaped film holder (see figures 1–3 in Denkov et al., 1996a). The diameter of the liquid film could be precisely controlled by sucking in or out (through a side capillary) some amount of the suspension, from which the film was formed. The film was observed by optical set-up, including an illuminating monochromatic light source and a long-focus magnifying lens. The liquid film thickness was determined from the intensity of the light reflected by the film (Scheludko, 1967). When the liquid film attained its desired thickness (~60 nm), it was plunged into a cooling liquid (1:1 mixture of ethane and propane, −190°C) for vitrification.

The advantages of the method used for sample preparation are 1) the vitrification is accomplished at the optimal film thickness (slightly larger than the vesicle diameter), thus ensuring better contrast of the images and absence of "flattening effect" (Dubochet et al., 1988), and 2) by controlling the film diameter, one can produce a well-ordered two-dimensional (2D) array of vesicles, which is suitable for further image analysis (Denkov et al., 1996b). The formation of a 2D array requires an appropriate vesicle concentration in the suspension used for film formation. We found by trial and error that a bR concentration of 0.22 mg/ml was most suitable for our purpose. Much lower concentrations of bR vesicles lead to the formation of a thin liquid film without vesicles inside, whereas slightly higher concentrations resulted in disordered mono- or multilayers of vesicles, which were not suitable for further image analysis. Such an adjustment of the bR concentration was performed only for the dialyzed samples; the nondialyzed samples were studied as obtained in the incubation procedure after removal of the precipitate (see the previous subsection and Fig. 1).

The frozen film was transferred into the electron microscope for observation at low temperature by means of CT 3500 cryo-transfer stage (Oxford Instruments). The shielding blades of the cryo-holder were opened at least 15 min after the insertion of the sample in the microscope to reduce ice condensation on the specimen. The observations of the samples were performed at −180°C and magnification 20K in a JEM-1200 EX JEOL transmission electron microscope (120 kV), equipped with an anticontaminator JEOL. The micrographs were taken with the minimum dose system to reduce the radiation damage, and highly sensitive negative films were used (MEM; Mitsubishi Paper Mills, Tokyo, Japan). The total electron dose of the samples was thus reduced to less than 200 e/nm^2.

The micrographs were digitized for image analysis by means of an automatic digitizer (Perkin-Elmer) at a resolution of 1.25 nm/pixel. The size of the images was ~1200 × 1200 nm, which corresponded to 500–700 vesicles in one image. The single-particle image analysis was performed at the Max Planck Institute for Biochemistry (Martinsried, Germany) on larger images digitized on a Leafscan 45 equipment (Leaf Systems, MA), with a resolution of 0.75 nm/pixel and containing up to 3800 vesicles.

RESULTS

Conditions of incubation at which vesicles are formed

As seen from Table 1, the vesicles spontaneously formed during the incubation at a variety of conditions. The pH of the solutions was varied between 5.2 and 8, the concentra-

tion of ammonium sulfate was varied from 0 to 1.25 M (thus changing the ionic strength of the solution as well), three different buffers were used (citrate, phosphate, and HEPES), and in all of these cases we obtained vesicles of practically the same size.

The most critical condition for obtaining bR vesicles was the ratio of the purple membrane and detergent (OTG) concentrations. To further clarify this point, we performed additional experiments in which the membrane concentration was varied between 0.3 and 7 mg/ml and the surfactant concentration between 0.2 and 10 mg/ml. The vesicle formation was quantified by monitoring whether crystals made up of spherical vesicles, like those observed by Kouyama et al. (1994), were produced when the detergent-membrane-salt mixtures were gradually concentrated by vapor diffusion (against a reservoir containing 1.9–2.1 M ammonium sulfate and 0.08 M sodium citrate at pH 5.2). As seen from Fig. 2, vesicular arrays were obtained only when the weight concentration of the protein was about twice that of the surfactant (see the two lines in Fig. 2 that enclose the region where vesicular crystals were formed). The excess of purple membrane resulted in the formation of a sediment of stacked flat membranes (due to the high ionic strength of the solutions). On the other side, the excess of OTG led to removal of the retinal from the bR molecules (Kouyama et al., manuscript submitted for publication) and to the formation of a sediment with an irregular, amorphous structure. We suppose that OTG of higher concentration caused a strong delipidation of the purple membrane and a partial denaturation of the protein molecules. Therefore, one can conclude that vesicles, which are photochemically active, are obtained only at an appropriate, relatively high ratio of protein to detergent (2:1 by weight).

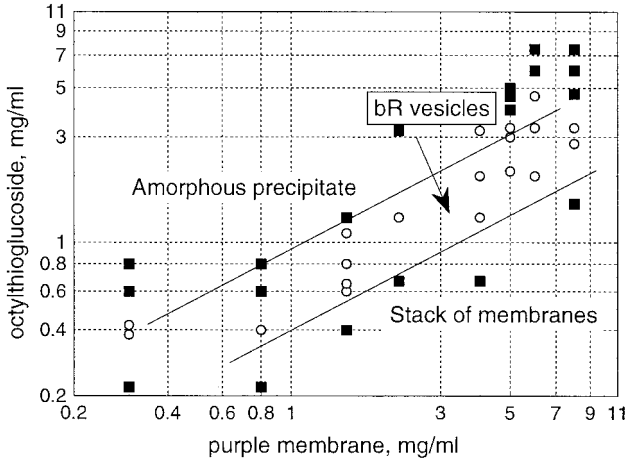

FIGURE 2 Diagram showing the concentration ranges where bR vesicles were formed. The two inclined lines are drawn as guides for the eye. The incubation of these samples was performed at pH 5.2 in the presence of 1.25 M ammonium sulfate, 50 mM sodium citrate, 0.14 M KCl, and 0.05% sodium azide.

Size and shape of the vesicles

The contrast in the micrographs of nondialyzed samples was very low because of the high concentration of salts in the aqueous medium. In samples 3 and 5, we were not able to see the vesicles clearly, even when the micrographs were taken at large underfocus or overfocus values (up to ± 10 μm). Therefore, we do not present data about the size of the vesicles before dialysis for these two samples. Nondialyzed samples 7 and 8 were not studied by cryomicroscopy. The vesicles in nondialyzed samples 1, 2, 4, and 6 could be seen at relatively large underfocus (see Fig. 3), and the average vesicle size was determined from digitized images by using a particle analysis software (Stanley Electric Co., Yokohama, Japan) (see Table 1). Between 60 and 150 vesicles were measured for each of the samples to determine the average radius and standard deviation. Remarkably, the average size of all nondialyzed samples fell within the narrow range between 17.9 and 19 nm, irrespective of the different conditions at which the vesicles were obtained (cf. the radii of samples 1Nd, 2Nd, 4Nd, and 6Nd in Table 1). The averaged value from all studied nondialyzed samples was 18.5 nm. On the other hand, the standard deviation within each sample was about ± 1.1 nm ($\pm 6\%$), i.e., the vesicles in a given sample showed a considerable variation in their size. In a given micrograph, one can easily distinguish vesicles that were substantially smaller or larger compared to the average size.

Many of the vesicles in the nondialyzed samples were ellipsoidal in shape, which indicated that these vesicles were rather deformable (this point is discussed in more detail in the second subsection of the Discussion, below). The aspect ratio (large to small axis) of the projections of the vesicles in the plane of the film was sometimes as large as 1.3. The precise determination of the radius of the vesicles was also hindered by the nonhomogeneous, grainy background of the micrographs (see Fig. 3), which was created by the presence

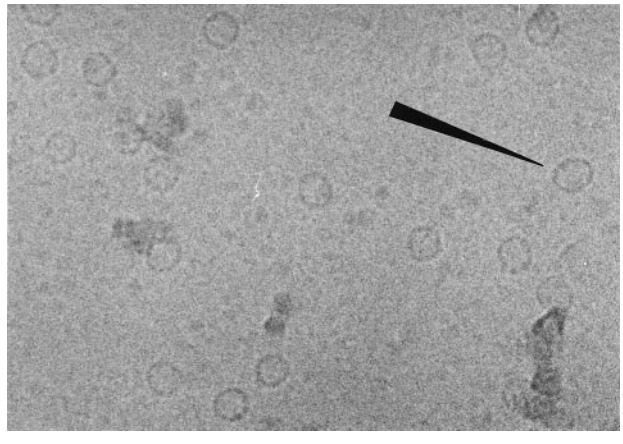

FIGURE 3 Cryoelectron micrograph of vesicles in vitrified film obtained from nondialyzed sample 6Nd. One vesicle of ellipsoidal shape is indicated by the arrow. The dark spots of irregular shape are crystals of cubic ice deposited as a contamination on the surface of the specimen.

of many micellar aggregates of OTG having a diameter of several nanometers.

The contrast of the micrographs from dialyzed images was substantially better, because of the lower salt concentration and the absence of OTG micelles. The size of 80–500 vesicles was measured in each sample, and the size distribution histograms were built (see Fig. 4, where the histogram of sample 2Dd is shown as an example). The size distribution of most samples could be well represented by normal distribution with a standard deviation close to ±1.0 nm. Sample 2Dd showed a somewhat narrower distribution (SD ±0.7 nm), but small and large vesicles were still easily perceptible. The average radius of all dialyzed samples fell in the interval between 14.7 and 16.7 nm. The radius of the vesicles in samples 7Dd and 8Dd (≈ 14.8 nm), which were obtained at pH 8, was slightly smaller than the average radius of the other dialyzed samples (≈15.9 nm), but it is difficult to decide whether this difference is statistically significant. On the other hand, the comparison of the radii of dialyzed and nondialyzed vesicles (see Table 1) clearly indicated that the vesicle radius diminished by ~2.5 nm upon dialysis. This value is well above the error of the size measurements and is rather reliable. On the other hand, the width of the size distribution remained practically the same (±1.0 nm). It is worth noting that the dialyzed vesicles appeared as spherical shells. No elliptically shaped vesicles, like that shown in Fig. 3, were seen. The damaged vesicles seemed like broken rigid shells rather than deformed flexible "balls." We interpret this observation as an indication that the dialyzed vesicles are substantially stiffer compared to the nondialyzed ones.

The implications of these results are reviewed in the Discussion.

Two-dimensional arrays and image analysis

Following the procedure described previously (Denkov et al., 1996a,b), we obtained more or less ordered, 2D arrays of vesicles in vitrified films from several of the samples. In most cases, however, the arrays were distorted because of the polydispersity of the vesicles and the procedure for vitrified film formation. These specimens were very convenient for vesicle size determination, but were inappropriate for refined image analysis.

We succeeded in obtaining a 2D array that was fairly regular and large in area from sample 2Dd (the one with narrowest size distribution) (see Fig. 5). The liquid film thickness just before vitrification was 59 nm. Micrographs were taken from this specimen at different underfocus and overfocus values (from −4 to +8 μm), and the average center-to-center distance between the vesicles in the array was measured as 44.7 nm. We did not observe electron diffraction spots from this sample, however, because the lattice constant of the vesicles in the array (44.7 nm) was too large to be detected.

From the size of the vesicles (R = 15.7) and the intervesicle distance, one can calculate the gap between two vesicles in the array to be ~3 nm (the thickness of the vesicle wall is 4.5–5 nm; Henderson and Unwin, 1975). One possible reason for this relatively large intervesicle separation could be the presence of a strong electrostatic repulsion between the charged walls of the vesicles. Such an electrostatic barrier would prevent the vesicles from direct contact, thus keeping them at a certain distance from each other. The equilibrium separation between charged particles is determined by the interplay of electrostatic and van der Waals forces acting between them, and typically appears at several times κ^{-1}, where κ is the inverse Debye screening length (see, e.g., section 12 in Israelachvili, 1992). One can estimate $\kappa^{-1} \approx 0.6$ nm in the studied solutions, which agrees with the measured intervesicle separation.

The micrographs of the ordered arrays were digitized, and a conventional 2D Fourier filtering of the images was accomplished to reduce the noise and to achieve image averaging. The numerical diffraction pattern showed significant spots of up to 6–7 nm (see the *inset* in Fig. 5). Accordingly, we could distinguish dark spots separated at a distance of ~7 nm in the central region of the average unit-cell structure (the average image of the vesicles) obtained by inverse Fourier transformation. However, the obtained structure depended on the particular place in the specimen, and on the size of the digitized image. These observations convinced us that the obtained arrays are not true 2D crystals, which is not surprising, keeping in mind the nonuniform size of the vesicles. Furthermore, the fine structure inside the "average" vesicle (discernible after the above "window filtering" procedure) obviously contained artefacts caused by the limited size of the analyzed images.

We proceeded further by trying single-particle, cross-correlation analysis. We collected vesicle images from the "best" negatives (including that shown in Fig. 5), and performed single-particle analysis on a data set containing more than 12,000 vesicles. However, this analysis did not

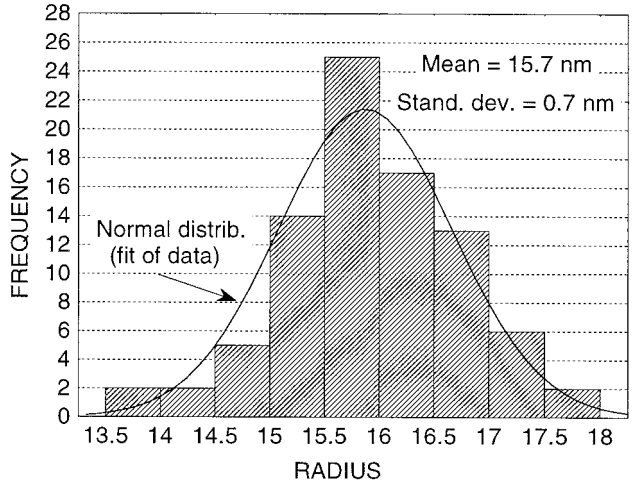

FIGURE 4 Size distribution histogram of the vesicles in sample 2Dd.

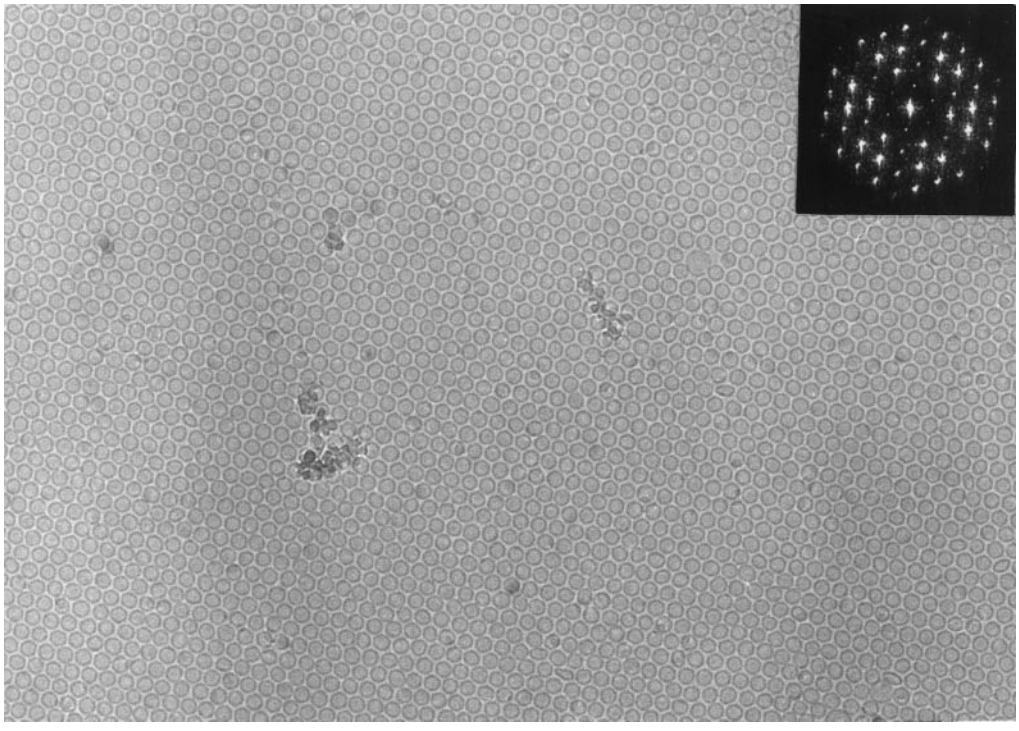

FIGURE 5 Two-dimensional array of vesicles from sample 2Dd. The mean intervesicle center-to-center distance is 44.7 nm. The inset shows the numerical Fourier transform of a digitized image containing 350 vesicles. The outermost spots correspond to 7-nm resolution in real space.

provide new structural information. Although some fine structure (dark spots separated from each other by 6–7 nm) could be discerned in the central part of many vesicles in the original images; the lateral and rotational alignment using different methods (single-reference or multireference alignment), as well as the eigenvector analysis and classification, did not reveal any characteristic structural motif.

Three main reasons for this negative result can be outlined: 1) the vesicles are rather variable in their fine structure, so that the averaging is not able to reveal a repeating motif; 2) the contrast in the central region is too low, because the thickness of the vitrified film is much larger compared to the protein shell; and 3) observation of the fine structure is prevented by the fact that the top and bottom regions of the vesicle wall are superimposed in the images.

DISCUSSION

Mechanism of vesicle formation and vesicle structure

Let us start with a summary of the experimental facts described in the Results:

1. The vesicles were spontaneously formed when purple membranes were incubated in the presence of OTG.
2. The vesicles were formed at a given ratio of the protein and surfactant (2:1).
3. All of the studied samples were of approximately the same size when compared either before or after dialysis (see Table 1).
4. All of the samples exhibited a certain vesicle size distribution with approximately the same standard deviation, $\sigma \approx \pm 1$ nm.
5. The vesicles shrunk in size upon dialysis and reduced their mean radius by 2–2.5 nm; the vesicles became stiffer after dialysis.

From other experiments (Kouyama et al., 1994, and manuscript submitted for publication) we know that 1) the bR retains its native, active conformation and the basic trimeric structure in the vesicles; 2) practically all of the bR molecules are oriented so that the cytoplasmic side (C-terminal end of the molecule) faces the external medium; and 3) the vesicles contain some native lipid—as shown by Wang and Kouyama (unpublished data), the vesicles contained the same number of phospholipid molecules per bR trimer before and after dialysis; there are no data for the glycolipid at present.

All of these facts considered together imply that the spontaneous bending of the purple membrane in the process of vesicle formation is due to a preferential incorporation of OTG molecules in the cytoplasmic side of the purple membrane (see Fig. 6). Indeed, the shrinking of the vesicles during dialysis is evidence that OTG molecules are removed from the vesicle membrane, after already being incorporated there during the incubation process. In addition, a

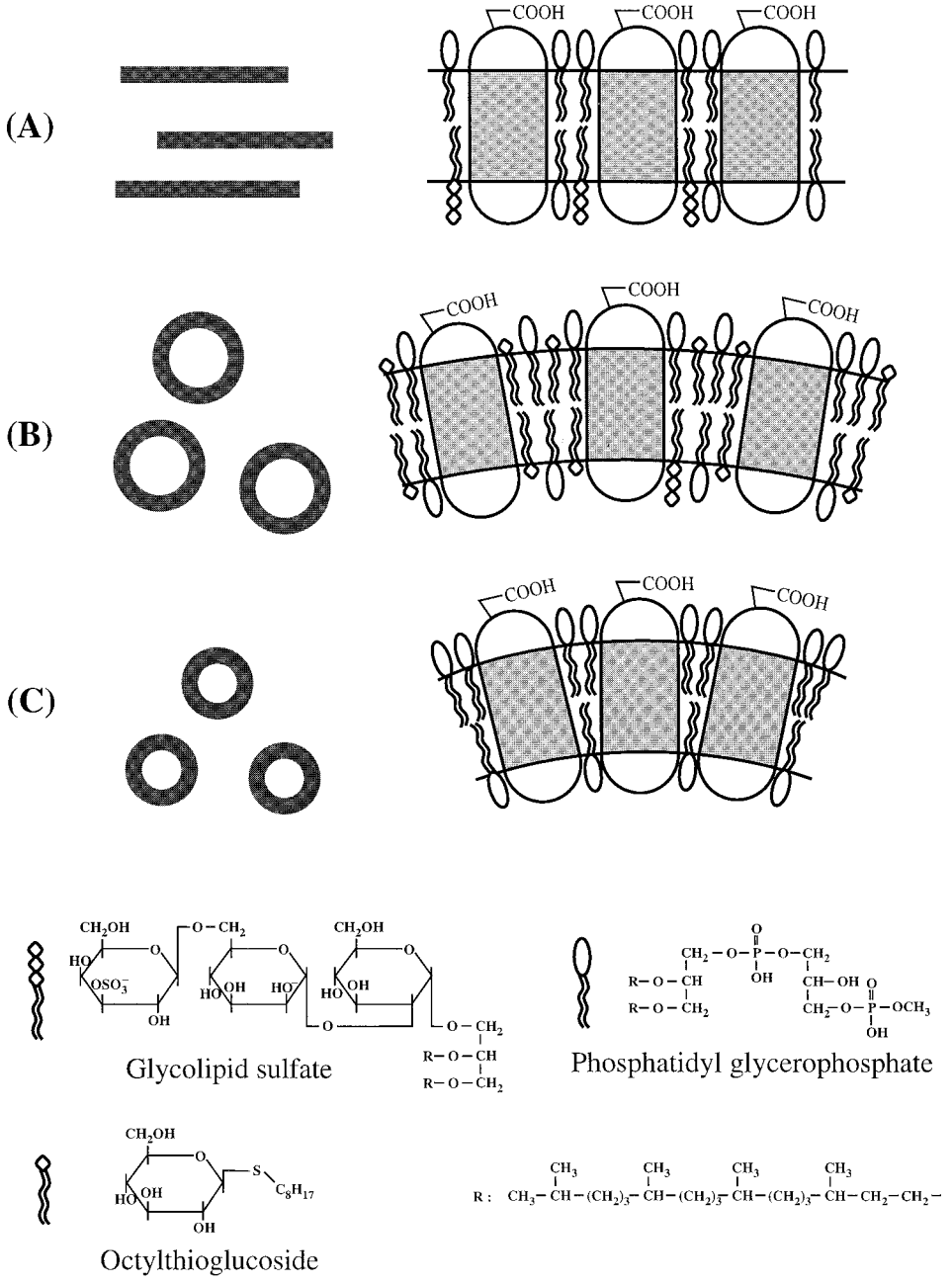

FIGURE 6 Schematic presentation of the processes of vesicle formation (*A* to *B*) and shrinking during dialysis (*B* to *C*).

preferential delipidation of the extracellular side could also take place during the incubation (Fig. 6), because of an inclusion of glycolipid sulfate molecules in the OTG micellar aggregates, but we have no data to prove (or to reject) this possibility at the present. Besides, the bR molecules possess an approximately constant cross section throughout the membrane thickness. Therefore, the concepts assuming conical proteins (Israelachvili, 1977, Israelachvili et al., 1980) could hardly be applied to explain the curvature of the bR vesicles.

On the other hand, the fact that the vesicle radius practically does not depend on pH and electrolyte concentrations (NaCl and ammonium sulfate), maintained during the incubation, means that the electrostatic interactions play a secondary role in the origin of the membrane curvature.

The phenomenon of asymmetrical incorporation of OTG molecules (and a possible asymmetrical delipidation of the purple membrane) could be anticipated, because the distribution of native lipids in the original purple membrane is known to be rather asymmetrical (Henderson et al., 1978; Ebrey, 1993). Almost all lipids in the cytoplasmic side of the membrane are phosphatidyl glycerophosphates (PGPs), the major component being the methyl ester PGP-Me (Tsujimoto et al., 1989; Kates et al., 1993). In the extracellular side, however, only about half of the lipids are glycerophosphates, whereas the remaining lipids are glycolipid sulfates

(Henderson et al., 1978; Kates et al., 1982; Grigorieff et al., 1996). A number of other experimental methods have demonstrated that asymmetry is an inherent property of the purple membrane (Zingsheim et al., 1978).

As mentioned above the dialyzed vesicles appeared as stiff spherical entities in the micrographs. Kouyama et al. (manuscript submitted for publication) have found that the vesicles become more stable mechanically after removal of the detergent by dialysis. Therefore, one could expect that the dialyzed vesicles comprise tightly packed bR trimers with some remaining lipid that fills the space between them. The number of the bR trimers per vesicle can be estimated from the sizes of the vesicles and bR. If we assume that one bR trimer occupies the same area in the vesicle as in the flat purple membrane (≈ 34 nm^2), one can estimate the number of trimers to be around 95 in a vesicle of radius $R = 16$ nm. This is an approximate figure, because the curvature of the vesicle surface is not taken into account. If we represent the shape of one bR trimer with a cylinder of diameter 6.27 nm and height 4.5 nm (Henderson and Unwin, 1975), and take into account the curvature of the vesicle shell, the estimated number is $\sim$25% smaller ($\approx$ 70 trimers per vesicle).

It is worth noting that the polydispersity of the vesicle radius in a given sample ($\pm$1 nm or $\pm$6%) corresponds to an appreciable variability in the vesicle area (on the order of $\pm$12%). One can estimate that the standard deviation of the number of bR trimers per vesicle within a given sample should be on the order of $\pm$10.

In some respects, the dialyzed vesicles could be compared with the polyhedral assembly of virus proteins in the closed viral shells. If we assume that the vesicles possess an icosahedral symmetry (similar to that found in viruses), the triangulation number that is closest to our structure is $T = 4$, corresponding to 80 quasiequivalent facets (Caspar and Klug, 1962). However, the structural analysis discussed above shows that our vesicles do not have an identical regular structure, which is typical for viruses. Moreover, the polydispersity of bR vesicles implies that their structure is not firmly restricted by the geometrical constraints that are so important for viruses. Therefore, the analogy between the structure of the bR vesicles and that of viruses is rather hypothetical, unless other arguments are found from future structural analysis.

On the other hand, the clathrin-coated and coatomer-coated vesicles in living cells appear to be much more polydisperse entities (Darnell et al., 1990; Alberts et al., 1994). This variability in biovesicle size could play some role in the regulation of the processes with respect to the size and amount of the substances that must be endocytosed or transported in the cell. Our results suggest that, in principle, such a variation in the vesicle size could be realized by incorporation of different lipids or lysolipids in the membrane (along with the membrane proteins), which would lead to different radii of spontaneous curvature.

As discussed above, the shrinkage of the vesicles upon dialysis is explained by desorption of OTG molecules from the vesicle wall (Fig. 6). The area of the vesicles diminishes by $\sim$400 nm^2 (25%) during this process, which corresponds to the surface occupied by OTG molecules before dialysis (a small number of OTG molecules may remain incorporated in the vesicles even after dialysis, but this is not taken into account in the following estimates). Assuming 0.4 nm^2 for the area per OTG molecule, one can estimate that $\sim$2000 OTG molecules are incorporated in the wall of one vesicle after the incubation (note that the OTG molecules are removed from both monolayers of the lipid bilayer). In other words, $\sim$20 OTG molecules per bR trimer are incorporated. In the original purple membrane we also have $\sim$30 lipid molecules per bR trimer (Fukuda et al., 1990; Grigorieff et al., 1996). Therefore, the large number of lipid and detergent molecules incorporated in the vesicle wall is responsible for the high flexibility of the nondialyzed vesicles (discussed above and in the next section).

In conclusion, our experimental results can be explained by a preferential incorporation of OTG molecules in the cytoplasmic side of the purple membrane, rather than by pure geometrical constraints created by the shape of the protein molecules. This preferential incorporation could be due to the asymmetrical distribution of the native lipids in the purple membrane and/or to some specific binding of the OTG molecules to the cytoplasmic side of bR. Further biochemical studies of the lipid composition of the bR vesicles could be rather helpful in formulating a clear picture of the protein-lipid complex in the vesicles.

Bending constant of nondialized bR vesicles

The experimental facts summarized in the beginning of the Discussion suggest that the polydispersity of the vesicles is a result of the flexibility of the purple membrane under incubation conditions. In other words, the variation in vesicle size in a given sample is a natural result of the fluctuations in the membrane curvature around the so-called spontaneous curvature (Helfrich, 1973; Israelachvili, 1992; Kralchevsky et al., 1994). Therefore, one can apply the thermodynamic theory of aggregation (Isrelachvili et al., 1980; Mitchell and Ninham, 1981; Israelachvili, 1992) and calculate the bending constant of the vesicle membrane.

In accordance with the thermodynamic approach, we consider each vesicle as an aggregate composed of N subunits (see Fig. 7). In our case, N presents the number of bR trimers (together with the adjacent lipid and surfactant molecules). In principle, N could be equal to 1, 2, 3, etc., to infinity, but in our samples N is always around 95, as discussed above. In equilibrium, the chemical potential of the protein molecules in all aggregates must be equal:

$$\mu_N = \mu_N^0 + \frac{kT}{N} \ln\left(\frac{X_N}{N}\right) = \text{const.} \qquad (1)$$

where μ_N is the chemical potential of a bR trimer in a vesicle containing N trimers in total; μ_N^0 is the standard part of the chemical potential that does not depend on the concentration of the aggregates (it depends, however, on the

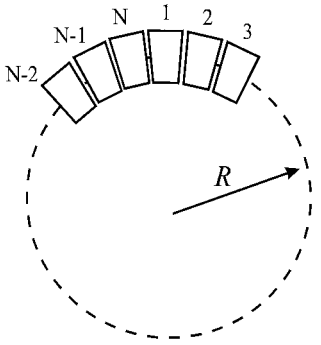

FIGURE 7 Schematic presentation of a vesicle of radius R, containing N bacteriorhodopsin trimers (together with the adjacent lipid and surfactant molecules). See Discussion for explanation.

temperature, pressure, and radius of the vesicle); kT is the thermal energy; and X_N is the total molar concentration of the bR trimers, which are captured in aggregates of type N. If M is the aggregation number corresponding to the mean size of the vesicles, than the probability of finding a vesicle of aggregation number N can be found as a direct consequence of Eq. 1 (see, e.g., Chapter 16 in Israelachvili, 1992):

$$\frac{X_N}{N} = \left\{\frac{X_M}{M}\exp\left[\frac{M(\mu_M^0 - \mu_N^0)}{kT}\right]\right\}^{N/M} \tag{2}$$

The standard chemical potential of the protein trimers in the vesicles depends primarily on the vesicle radius, R, at constant temperature and pressure. Therefore, we can write (see Chapter 17 in Israelachvili, 1992)

$$N\mu_N^0 = N\mu_M^0 + 4\pi R^2 W_B \tag{3}$$

where W_B is the bending elasticity energy per unit area of the membrane. According to Helfrich (1973), W_B can be presented in the form (for small deviations from the spontaneous curvature)

$$W_B = \frac{K_B}{2}\left(\frac{1}{R} - \frac{1}{R_0}\right)^2 \tag{4}$$

where K_B is the so-called bending elasticity constant and R_0 is the radius of spontaneous curvature (we assume that R_0 is equal to the mean vesicle radius in the sample). Note that Eq. 4 is written in accordance with the definition of bending energy used by Israelachvili (1992). The bending energy in the original theory (Helfrich, 1973) was defined with the numerical factor 2 in the numerator, rather than in the denominator, as it is in Eq. 4. Therefore, the bending elasticity constant in Helfrich's notation is four times smaller than K_B. Combining Eqs. 2–4, we obtain

$$C_N = \left\{C_M\exp\left[-\frac{M}{N}\frac{2\pi K_B}{kT}\left(1 - \frac{R}{R_0}\right)^2\right]\right\}^{N/M} \tag{5}$$

where $C_N \equiv X_N/N$ is the molar concentration of the aggregates containing N protein trimers. Taking into account the fact that the area of the vesicles is proportional to the number of bR trimers,

$$N = 4\pi R^2/A_0 \text{ and } M = 4\pi R_0^2/A_0 \tag{6}$$

(A_0 is the area per one bR trimer), one can rewrite Eq. 5 in the form

$$C_N = \left\{C_M\exp\left[-\frac{2\pi K_B}{kT}\left(1 - \frac{R_0}{R}\right)^2\right]\right\}^{R^2/R_0^2} \tag{7}$$

which represents the size distribution of the aggregates in the sample, according to the adopted model. Equation 7 can be further simplified, taking into account the fact that the polydispersity in our samples is small, $(1 - R/R_0)^2 \ll 1$. By expanding the right-hand side of Eq. 7 in series around the radius of spontaneous curvature, and keeping the leading terms, one obtains

$$C(R) \approx C(R_0)\exp\left[-\frac{2\pi K_B}{kT}\left(\frac{R - R_0}{R_0}\right)^2\right] \tag{8}$$

Equation 8 predicts that the vesicles are normally distributed in size around the average radius, R_0, and that the standard deviation in the vesicle radius, σ, can be expressed as

$$\sigma^2 = \frac{kT}{4\pi K_B}R_0^2 \tag{9}$$

Therefore, the bending elasticity constant, K_B, can be estimated from the experimentally accessible values of the mean vesicle radius, R_0, and the standard deviation, σ:

$$K_B = \frac{kT}{4\pi}\left(\frac{R_0}{\sigma}\right)^2 \tag{10}$$

Taking typical values for nondialyzed vesicles from our experiments ($R_0 = 18$ nm, $\sigma = 1.1$ nm), we calculate from Eq. 10 that $K_B/kT \approx 21$ ($K_B = 0.87 \times 10^{-19}$ J). This value is very close to the values that were experimentally obtained for lipid bilayers in the fluid state by several methods (see, e.g., Evans and Rawicz, 1990; Israelachvili, 1992). This result confirms our observation that the nondialyzed vesicles are rather flexible (see Results), and it shows that the bending rigidity of the vesicle membrane is comparable with that of the fluid lipid bilayers. Note that the numerical factor in the denominator in the right-hand side of Eq. 10 would be 16π (instead of 4π) if we adopt the Helfrich definitions of the bending energy and elasticity constant. Thus the calculated bending elasticity constant is equal to $\sim 5kT$ in the Helfrich notation.

The above consideration is applicable only to nondialyzed vesicles, because they are spontaneously formed during the incubation, and their size distribution corresponds to the equilibrium distribution. As discussed in the previous section, the dialyzed vesicles are stiffer because of the removal of detergent molecules from the vesicle wall. We could not estimate the bending elasticity constant of the dialyzed samples by the above procedure, because the size

distribution in these samples is "inherited" from the primary, nondialyzed samples, and it is a nonequilibrium distribution.

CONCLUSIONS

In the present study we show that bR vesicles can be formed from purple membrane at different compositions of the original suspension, but only if the protein:OTG ratio is ~2:1 (Fig. 2). The size distribution of the vesicles is practically independent of the conditions under which the vesicles are obtained, $R \approx 18.5 \pm 1.1$ nm (Table 1 and Fig. 4). The spontaneous formation of the vesicles is explained by a preferential incorporation of OTG molecules into the cytoplasmic side of the purple membrane during its incubation at elevated temperature (Fig. 6). From the electron cryomicroscopy images, one can see that the vesicles are rather deformable (Fig. 3). By using the thermodynamic theory of aggregation (Israelachvili et al., 1980), we calculated the bending elasticity constant, $K_B = 0.87 \times 10^{-19}$ J, from the vesicle size distribution. This value is very close to the values for fluid lipid bilayers reported in the literature.

The dialysis of the vesicle suspensions for the removal of OTG leads to shrinking of the vesicles due to desorption of the detergent from the vesicle walls (Table 1 and Fig. 6). As a result, the vesicles become stiffer and probably comprise tightly packed bR trimers. A well-ordered two-dimensional array of dialyzed vesicles was produced from one of the samples (Fig. 5), and the micrographs obtained were analyzed in an attempt to retrieve more detailed information about the vesicle structure. The averaging of the images of different vesicles, however, did not reveal one or several structural motifs. The latter result is most probably due to the high variability of the vesicle structure.

The present results are in very good agreement with (and complement) the results of other studies (Kouyama et al., 1994, and manuscript submitted for publication). For instance, the nonuniform size distribution of the vesicles, measured by us, explains why the x-ray diffraction from the 3D arrays of vesicles did not provide fine structural information.

The driving force of the purple membrane bending, discussed above (and the resulting vesicle formation), deserves further investigation. The fact that Tributsch and Bogomolni (1994) succeeded in forming similarly sized vesicles (details about their structure are not available at present) by using a different experimental procedure and azolectin lipids instead of OTG suggests that the mechanism of asymmetrical incorporation of lipids (or lysolipids and detergents) could be more universal. It would be interesting to check whether other protein-containing membranes could spontaneously form vesicles in this way, and to analyze the extent to which this mechanism takes place in biological cells.

The authors are thankful to Professor W. Baumeister (Max Planck Institute for Biochemistry, Martinsried, Germany) for the helpful suggestions concerning the single-particle image analysis. The vesicle size determination for several of the samples was performed by Mr. Fumio Kubo (Stanley Electric Co., Yokohama, Japan).

This study was performed under the program Exploratory Research for Advanced Technology (ERATO, JRDC).

REFERENCES

Alberts, B., D. Bray, J. Lewis, M. Raff, K. Roberts, and J. D. Watson. 1994. Molecular Biology of the Cell, 3rd ed. Garland Publishing, New York.

Birge, R. R. 1994. Bacteriorhodopsin: a nonlinear proton pump. *Nature.* 371:659–660.

Branden, C., and J. Tooze. 1991. Introduction to Protein Structure. The structure of spherical viruses, pp. 161–177. Garland Publishing, New York.

Caspar, D. L. D., and A. Klug. 1962. Physical principles in the construction of regular viruses. *Cold Spring Harb. Symp. Quant. Biol.* 27:1–24.

Darnell, J. E., H. Lodish, and D. Baltimore. 1990. Molecular Cell Biology, 2nd ed. Scientific American Books, New York.

Denkov, N. D., H. Yoshimura, and K. Nagayama. 1996a. Method for controlled formation of vitrified films for cryo-electron microscopy. *Ultramicroscopy.* 65:147–158.

Denkov, N. D., H. Yoshimura, K. Nagayama, and T. Kouyama, 1996b. Nanoparticle arrays in freely suspended vitrified films. *Phys. Rev. Lett.* 76:2354–2357.

Dubochet, J., M. Adrian, J.-J. Chang, J.-C. Homo, J. Lepault, A. W. McDowall, and P. Schultz. 1988. Cryo-electron microscopy of vitrified specimens. *Q. Rev. Biophys.* 21:129–228.

Ebrey, T. 1993. Light energy transduction in bacteriorhodopsin. *In* Thermodynamics of Membrane Receptors and Channels. M. B. Jackson, editor. CRC Press, Boca Raton, FL. 353–387.

Evans, E., and W. Rawicz. 1990. Entropy-driven tension and bending elasticity in condensed-fluid membranes. *Phys. Rev. Lett.* 64: 2094–2097.

Fukuda, K., A. Ikegami, A. Nasuda-Kouyama, and T. Kouyama. 1990. Effect of partial delipidation of purple membrane on the photodynamics of bacteriorhodopsin. *Biochemistry.* 29:1997–2002.

Grigorieff, N., T. A. Ceska, K. H. Downing, J. M. Baldwin, and R. Henderson. 1996. Electron-crystallographic refinement of the structure of bacteriorhodopsin. *J. Mol. Biol.* 259:393–421.

Harrison, S. C. 1984. Multiple modes of subunit association in the structures of simple spherical viruses. *Trends Biochem. Sci.* 9:345–351.

Helfrich, W. 1973. Elastic properties of lipid bilayers: theory and possible experiments. *Z. Naturforsch. C.* 28:693–703.

Henderson, R. 1975. The structure of the purple membrane from *Halobacterium halobium*: analysis of the x-ray diffraction pattern. *J. Mol. Biol.* 93:123–138.

Henderson, R., J. M. Baldwin, T. A. Ceska, F. Zemlin, E. Beckmann, and K. H. Downing. 1990. Model for the structure of bacteriorhodopsin based on high-resolution electron cryo-microscopy. *J. Mol. Biol.* 213: 899–929.

Henderson, R., J. S. Jubb, and S. Whytock. 1978. Specific labelling of the protein and lipid on the extracellular surface of purple membrane. *J. Mol. Biol.* 123:259–274.

Henderson, R., and D. Shotton. 1980. Crystallization of purple membrane in three dimensions. *J. Mol. Biol.* 139:99–109.

Henderson, R., and P. N. T. Unwin. 1975. Three-dimensional model of purple membrane obtained by electron microscopy. *Nature.* 257:28–32.

Horne, R. W. 1979. The formation of virus crystalline and paracrystalline arrays for electron microscopy and image analysis. *Adv. Virus Res.* 24:173–221.

Horne, R. W., and I. Pasquali-Ronchetti. 1974. A negative staining carbon film technique for studying viruses in the electron microscope. I. Preparation procedures for examining icosahedral and filamentous viruses. *J. Ultrastruct. Res.* 47:361–383.

Israelachvili, J. N. 1977. Refinement of the fluid-mosaic model of membrane structure. *Biochim. Biophys. Acta.* 469:221–225.

Israelachvili, J. N. 1992. Intermolecular and Surface Forces, 2nd ed. Academic Press, New York.

Israelachvili, J. N., S. Marcelja, and R. G. Horn. 1980. Physical principles of membrane organization. *Q. Rev. Biophys.* 13:121–200.

Kates, M., S. C. Kushwaha, and G. D. Sprott. 1982. Lipids of purple membrane from extreme halophiles and of methanogenic bacteria. *Methods Enzymol.* 88:98–111.

Kates, M., N. Moldoveanu, and L. C. Stewart. 1993. On the revised structure of the major phospholipid of *Halobacterium salinarium. Biochim. Biophys. Acta.* 1169:46–53.

Kelly, R. B. 1993. Storage and release of neurotransmitters. *Cell Neuron.* 72:43–53.

Khorana, H. G. 1988. Bacteriorhodopsin, a membrane protein that uses light to translocate protons. *J. Biol. Chem.* 263:7439–7442.

Kimura, Y., D. G. Vassylyev, A. Miyazawa, A. Kidera, M. Matsushima, K. Mitsuoka, K. Murata, T. Hirai, and Y. Fudjiyoshi. 1997. Surface of bacteriorhodopsin revealed by high-resolution electron crystallography. *Nature.* 389:206–211.

Klug, A., and D. L. D. Caspar. 1960. The structure of small viruses. *Adv. Virus Res.* 7:225–325.

Kouyama, T., M. Yamamoto, N. Kamiya, H. Iwasaki, T. Ueki, and I. Sakurai. 1994. Polyhedral assembly of a membrane protein in its three-dimensional crystal. *J. Mol. Biol.* 236:990–994.

Kralchevsky, P. A., J. C. Eriksson, and S. Ljunggren. 1994. Theory of curved interfaces and membranes: mechanical and thermodynamical approaches. *Adv. Colloid Interface Sci.* 48:19–59.

Kreis, T. E. 1992. Regulation of vesicular and tubular membrane traffic of the Golgi complex by coat proteins. *Curr. Opin. Cell Biol.* 4:609–615.

Kühlbrandt, W. 1988. Three-dimensional crystallisation of membrane proteins. *Q. Rev. Biophys.* 21:429–477.

Ladenstein, R., M. Shneider, R. Huber, H.-D. Bartunik, K. Wilson, K. Schott, and A. Bacher. 1988. Heavy riboflavin synthase from *Bacillus subtilis*: crystal structure analysis of the icosahedral β_{60} capsid at 3.3 Å resolution. *J. Mol. Biol.* 203:1045–1070.

Michel, H. 1982. Characterization and crystal packing of three-dimensional bacteriorhodopsin crystals. *EMBO J.* 1:1267–1271.

Michel, H., and D. Oesterhelt. 1980. Three-dimensional crystals of membrane proteins: bacteriorhodopsin. *Proc. Natl. Acad. Sci. USA.* 77: 1283–1285.

Mitchell, D. J., and B. W. Ninham. 1981. Micelles, vesicles and microemulsions. *J. Chem. Soc. Faraday Trans.* 277:601–629.

Oesterhelt, D., and W. Stoeckenius. 1973. Functions of a new photoreceptor membrane. *Proc. Natl. Acad. Sci. USA.* 70:2852–2857.

Oesterhelt, D., and W. Stoeckenius. 1974. Isolation of the cell membrane of *Halobacterium halobium* and its fragmentation into red and purple membrane. *Methods Enzymol.* 31:667–678.

Orci, L., D. J. Palmer, M. Amherdt, and J. A. Rothman. 1993. Coated vesicle assembly in the Golgi requires only coatomer and ARF proteins from the cytosol. *Nature.* 364:732–734.

Pearse, B. M. F., and R. A. Crowther. 1987. Structure and assembly of coated vesicles. *Annu. Rev. Biophys. Biophys. Chem.* 16:49–68.

Rehorek, M., and M. P. Heyn. 1979. Binding of all-trans-retinal to the purple membrane: evidence for cooperativity and determination of the extinction coefficient. *Biochemistry.* 18:4977–4983.

Sakata, K., Y. Kimura, and Y. Fujiyoshi. 1992. Methods for orienting purple membrane in vitreous ice. *Bull. Inst. Chem. Res. Kyoto Univ.* 70:257–269.

Scheludko, A. 1967. Thin liquid films. *Adv. Colloid Interface Sci.* 1:392–470.

Schertler, G. F. X., H. D. Bartunik, H. Michel, and D. Oesterhelt. 1993. Orthorombic crystal form of bacteriorhodopsin nucleated on benzamidine diffracting to 3.6 Å resolution. *J. Mol. Biol.* 234:156–164.

Takeda, S., H. Yoshimura, S. Endo, T. Takahashi, and K. Nagayama. 1995. Control of crystal forms of apoferritin by site-directed mutagenesis. *Proteins Struct. Funct. Genet.* 23:548–556.

Tributsch, H., and R. A. Bogomolni. 1994. Bacteriorhodopsin: a molecular photooscillator? *Chem. Phys. Lett.* 227:74–78.

Tsujimoto, K., S. Yorimitsu, T. Takahashi, and M. Ohashi. 1989. Revised structure of a phospholipid obtained from *Halobacterium halobium. J. Chem. Soc. Chem. Commun.* 1:668–670.

Unwin, P. N. T., and R. Henderson. 1975. Molecular structure determination by electron microscopy of unstained crystalline specimens. *J. Mol. Biol.* 94:425–440.

Zingsheim, H. P., D.-Ch. Neugebauer, and R. Henderson. 1978. Properties of the two sides of the purple membrane correlated. *J. Mol. Biol.* 123:275–278.